A novel fluorescence sensing system using a photochromism-based assay (P-CHROBA) technique for the detection of target proteins

Kin-ya Tomizaki and Hisakazu Mihara*

Received 4th February 2005, Accepted 17th March 2005
First published as an Advance Article on the web 6th April 2005
DOI: 10.1039/b501877n

In the post-genomic era a number of biological technologies, including protein-detecting microarrays which can detect molecular interactions based on changes in fluorescence intensity, have been developed to investigate complicated protein functions and networks. However, the ability of such techniques to obtain reproducible and quantitative results can be compromised due to the need for the immobilization of capture agents and the labelling analytes with chromophores. In the present study, first we report the design and synthesis of photochromic spiropyran-containing peptides and then demonstrate a unique fluorescence sensing system comprising a photochromism-based assay (P-CHROBA) technique to distinguish between target proteins. The spiropyran moiety in the peptides exhibited characteristic physicochemical properties in the SP-to-MC isomerization (thermocoloration) and the MC-to-SP photoisomerization (photobleaching) depending upon changes in micro-environments such as the dielectric constants of solvents and steric hindrances generated by molecular interactions. We attempted to detect protein–peptide interactions using reproducible MC-to-SP photoisomerization properties by monitoring the fluorescence decay of the MC form in the peptide. This can reduce background fluorescence signals caused by emission from excess reagents and avoid the laborious introduction of probing molecules to analytes and the immobilization of capture agents onto solid surfaces. The protein fingerprints (PFPs) based on the photoisomerization properties could successfully distinguish between six different model proteins, and the combination of the P-CHROBA and PFP technique would be a powerful tool for profiling target proteins with reproducible and reliable results.

Introduction

The complete genome sequencing of various organisms has allowed us to obtain a large amount of valuable information for understanding complex cellular events. Consequently, a number of biological technologies including oligonucleotide arrays and protein-detecting microarrays have been emerging with increasing frequency. The oligonucleotide arrays, which provide important information on changes in mRNA expression levels in response to a variety of physiological stimuli, are now commercially available and are a promising tool for analyzing gene expression.[1] Protein-detecting microarrays, which can detect antigen–antibody, protein–protein, protein–ligand, protein–saccharide, and protein–small molecule interactions, will become a powerful biological research tool in the near future.[2] However, the protein-detecting microarrays need to meet several requirements: ease of manipulation; a competitive price; highly sensitive labelling reagents, and for an efficient detection method to be developed for practical protein-detecting chips. From this point of view, dozens of exciting reviews on protein-detecting microarrays have been reported in past few years.[3–17] Today, antibodies are the most promising capture agents for detecting target proteins and for antibody chips, where antibodies are immobilized onto glass plates, and have just been released commercially.[18,19] However, methods for the production of highly potent antibodies must be developed because a number of antibodies corresponding to the target proteins is required. We have previously designed and synthesized fluorophore-containing peptide libraries with secondary structures such as the α-helix,[20] β-strand,[21] and β-loop.[22] We have demonstrated that they can be used to distinguish between proteins of interest using protein fingerprints (PFPs) which are based on changes in the fluorescence intensity characteristic of complexes formed by the protein–peptide interactions. Our PFP technique does not require the antibodies and/or the analytes to be labelled with a chromophore because the dyes have already been site-specifically incorporated into the peptide chains by a synthetic chemical method. Although a protein-detection system is currently available, it requires improvements such as a reduction in the relatively high background signals resulting from modification of the capture agents with chromophores. One means of improving the PFP technique is to alter the wavelengths of the fluorescence maxima of the protein–peptide interactions. Another way is to use measurements which are independent of the background fluorescence signals from excess reagents. Thus, desirable labelling groups of this kind could be exploited to probe the surfaces of proteins of interest and to make the emerging PFP technique more broadly applicable.

Spiropyrans, well known photochromic compounds, have been vigorously studied in the field of molecular switches and memories.[23] Each spiropyran derivative has an equilibrium

*hmihara@bio.titech.ac.jp

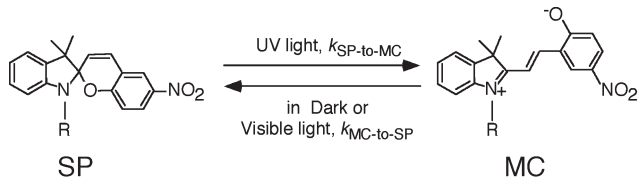

Fig. 1 Photochromic properties of spiropyran derivatives in common organic solvents. The spiropyran (SP) form can be converted to the merocyanine (MC) form by UV light irradiation with a photoisomerization rate constant, $k_{SP\text{-}to\text{-}MC}$, also the MC form can be isomerized by darkness, or by visible light irradiation with a rate constant, $k_{MC\text{-}to\text{-}SP}$.

constant between that of the fluorescent merocyanine (MC) form (colored in pink) and the non-fluorescent colorless spiropyran (SP) form characteristic of the dielectric constant of solvents.[24] The chemical structure of spiropyrans in common organic solvents can be controlled by UV and visible light irradiation or UV light and incubation in the dark (Fig. 1).[25] Using such unique photochromic properties, spiropyrans have been employed not only in materials chemistry but also in bio-organic chemistry, especially as an analytical tool for the transport of amino acid derivatives across bilayers or membranes,[26] or as capture agents for amino acids on the surface of gold nanoparticles[27] indicating that the photomerocyanine form of the spiropyran derivatives is able to recognize appropriately charged molecules *via* electrostatic interactions. The MC-to-SP isomerization properties of spiropyran derivatives are also affected by the sterically-hindered environments present in organogels.[23b,28]

Recently, we have successfully demonstrated a chromism-based assay (CHROBA) technique for the *in situ* detection of the protein kinase A (PKA)-catalyzed phosphorylation, based on changes in the thermocoloration from the colorless SP-form to the fluorescent MC-form, depending upon the phosphorylation of a serine side chain in the spiropyran-containing peptide substrate.[29] This technique offers a system that reduces the influence of background signals from reagents, does not require the immobilization of the peptide substrates, isotope-labeled ATP and specific anti-phosphoamino acid antibodies, and thus facilitates production and manipulation. However, the method based on the chromic properties of spiropyrans appears to be an early stage in the evolution of a promising technology for detecting molecular interactions. In order to extend the applicability of this technique, we report herein the first example of a photochromism-based assay (P-CHROBA) technique for profiling proteins of interest in which, the MC-to-SP photoisomerization rate constants that are characteristic of changes in the micro-environments surrounding a spiropyran moiety in peptides are utilized as a factor to distinguish between proteins in complexes.

Results and discussion

Design and synthesis of spiropyran-containing peptides

The rationale behind the design of a novel protein-detecting system using spiropyran-containing peptides is based on the photophysical properties of a spiropyran moiety varying between a colorless "closed" SP-form and a highly colored "open" MC-form, these transitions being controllable by UV and visible light irradiation (and sometimes incubation in the dark). The amino acid sequences of peptides were chosen from the substrates of four different kinases [protein kinase A (PKA),[30] c-Src kinase,[31] c-Abl tyrosine kinase,[31] and protein kinase C (PKC)[32]] having a relatively similar charge balance but different arrangement of amino acid components (Fig. 2). The spiropyran derivative was attached to the side chain of lysine (for K-PKA-SP (**1**), K-cSrc-SP (**6**), K-cAbl-SP (**7**), and K-PKC-SP (**8**)), ornithine (for O-PKA-SP (**2**)), L-α,γ-diaminobutyric acid (Dab) (for Db-PKA-SP (**3**)), and L-α,β-diaminopropionic acid (Dap) (for Dp-PKA-SP (**4**)), all of which were placed at the *N*-terminus of the interaction site through a glycine spacer. An *S*-protected cysteine residue was attached to the *N*-terminus of the sequence for future conjugation with another functional group. All peptides were capped with an acetyl (Ac) group at their *N*-termini, except Nt-PKA-SP (**5**) in which the *N*-terminus was modified with the spiropyran derivative.

The eight spiropyran-containing peptides were prepared *via* three different synthetic routes (Scheme 1). In routes 1 and 3, the spiropyran moiety is incorporated into the side chain or *N*-terminus of the full length peptide on the resin after completion of the peptide chain elongation by solid phase synthesis. In route 2, spiropyran-tethered Fmoc-amino acids are prepared in advance and then employed in the common solid phase peptide synthesis. First, the known spiropyran derivative, 2-(3′,3′-dimethyl-6-nitro-3′*H*-spiro[chromene-2,2′-indole]-1′-yl)ethanol (**9**) was prepared from commercially

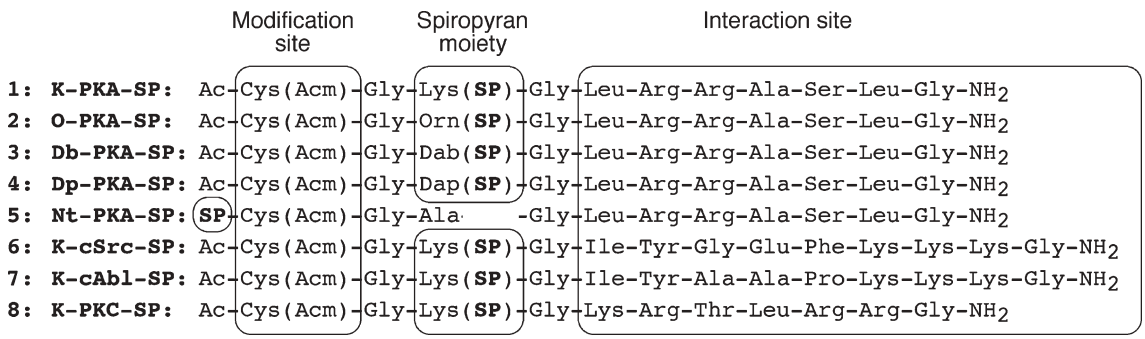

Fig. 2 Amino acid sequences of spiropyran-containing peptides comprosed of three parts: a modification site, a spiropyran moiety, and an interaction site. 'SP' denotes the spiropyran moiety.

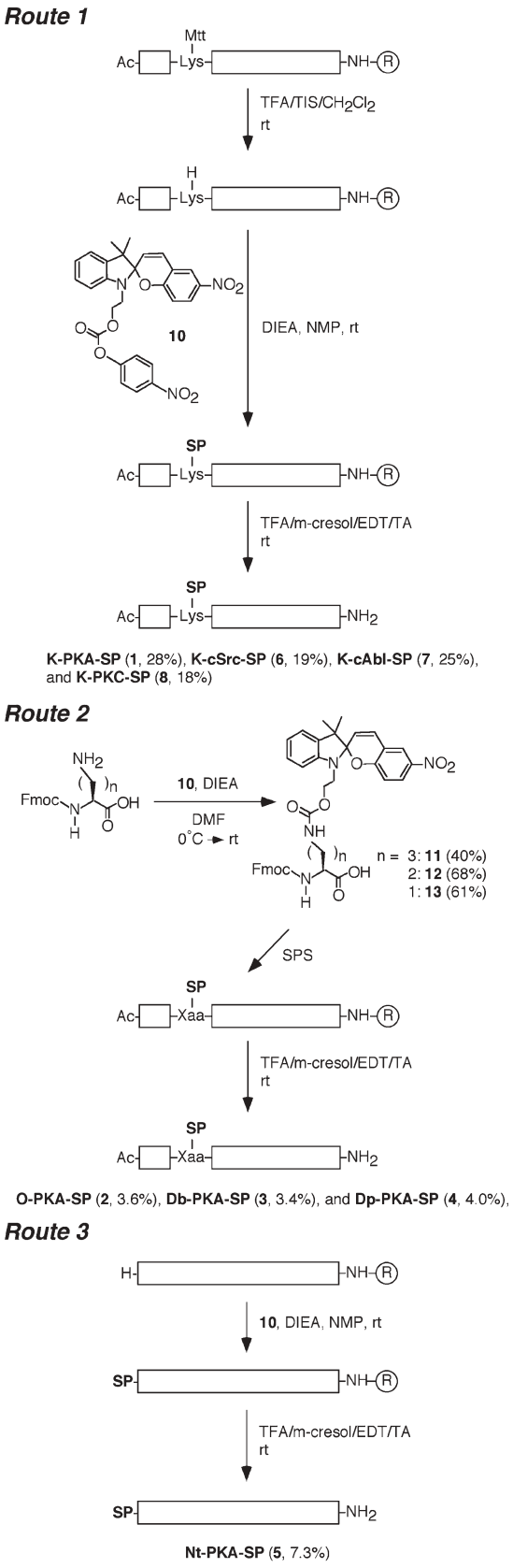

Scheme 1 Synthesis of spiropyran-containing peptides *via* three different routes.

available 2,3,3-trimethyl-3*H*-indole *via* three steps resulting in ~50% overall yield.[25] Compound **9** was treated with *p*-nitrophenyl chloroformate, giving an activated spiropyran (**10**) with 56% yield. In route 1 for preparation of K-PKA-SP (**1**), K-cSrc-SP (**6**), K-cAbl-SP (**7**), and K-PKC-SP (**8**), after completion of the peptide chain elongation by solid phase synthesis using Fmoc chemistry,[33] the 4-methyltrityl (Mtt) group protecting the lysine side chain was removed with trifluoroacetic acid (TFA)/triisopropylsilane (TIS)/CH_2Cl_2 (1/5/94, v/v/v). Compound **10** was reacted with the generated amino group in the peptides. In route 2 for preparation of O-PKA-SP (**2**), Db-PKA-SP (**3**), and Dp-PKA-SP (**4**), the Fmoc-L-α-amino acids tethering a spiropyran moiety to the ω-amino groups were synthesized by coupling **10** with an ω-free amino group in Fmoc-L-α-amino acids, giving compounds **11**, **12**, and **13** with 40, 68, and 61% yield, respectively. The Fmoc-L-α-amino acids tethering the spiropyran moiety were used in the usual solid phase peptide synthesis by the Fmoc strategy.[33] In route 3 for Nt-PKA-SP (**5**), the spiropyran derivative was connected to the *N*-terminus of the sequence on the resin. The fully-protected peptide-bound resins were treated with TFA/*m*-cresol/ethanedithiol (EDT)/thioanisole (TA) (40/1/3/3, v/v/v/v) at room temperature and the crude peptides obtained were purified by reversed phase high performance liquid chromatography (RP-HPLC), followed by lyophilization, giving pure compounds as a yellow powder with 28% yield for K-PKA-SP (**1**), 3.6% for O-PKA-SP (**2**), 3.8% for Db-PKA-SP (**3**), 4.0% for Dp-PKA-SP (**4**), 7.3% for Nt-PKA-SP (**5**), 19% for K-cSrc-SP (**6**), 25% for K-cAbl-SP (**7**), and 18% for K-PKC-SP (**8**). Molecular ion peaks for all peptides were observed by matrix-assisted laser desorption/ionization time-of-flight mass spectrometry (MALDI-TOFMS). Yields of some peptides, especially O-PKA-SP (**2**), Db-PKA-SP (**3**), and Dp-PKA-SP (**4**) synthesized *via* route 2 were significantly lower than for others, probably due to incomplete introduction of spiropyran-tethered Fmoc-amino acids and/or side reactions of the spiropyran moiety during the peptide chain elongation. Therefore, route 1 would be a better way to synthesize spiropyran-containing peptides by the solid phase technique.

SP-to-MC thermocoloration properties of spiropyran-containing peptides

First, we investigated photochromic properties of spiropyran-containing peptides in neutral aqueous media, then employed them to profile proteins of interest using the MC-to-SP photoisomerization rate constants as a probing factor.

When the yellow powder, colored by a co-existing protonated MC-form, was dissolved in a neutral aqueous solution the yellow solution immediately turned pink due to deprotonation of the phenolic proton of the MC moiety, resulting in the fluorescent zwitterion MC-form. Fig. 3A shows the absorption and fluorescence spectra of K-PKA-SP (**1**) in aqueous buffered solution acquired immediately after preparation of the sample solution. An intense visible absorption band at 510 nm and fluorescence emission at 600 nm (λ_{ex} = 510 nm) were observed in the absorption and fluorescence spectra, respectively, indicating a mixture of the SP and MC forms in the spiropyran moiety. The absorption

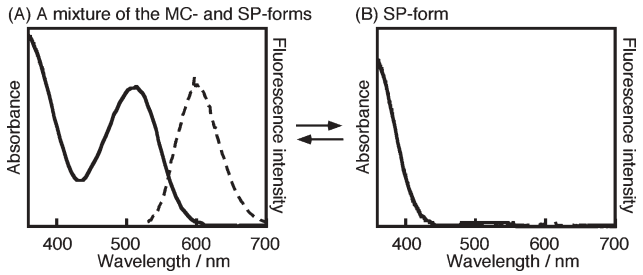

Fig. 3 Absorption (solid lines) and fluorescence (dashed lines, λ_{ex} = 510 nm) spectra of K-PKA-SP (**1**) taken immediately after dissolving the yellow powder in 20 mM Tris HCl buffer (pH 7.4) (A) and after completion of photoisomerization by irradiation with 510 nm light for 30 min at 25 °C (B).

and fluorescence spectra of the SP-form in the K-PKA-SP (**1**) solution taken after irradiation with 510 nm light for 30 min at 25 °C are shown in Fig. 3B. Both the intense absorption band at 510 nm and the fluorescence emission at 600 nm disappeared on completion of the MC-to-SP photoisomerization. When the solution containing predominantly the SP-form was incubated in the dark at room temperature for several hours it turned pink again, indicating that the chemical structure of the spiropyran moiety in K-PKA-SP (**1**) is reversibly controlled by visible light for the MC-to-SP photoisomerization (photobleaching) and by incubation in the dark for the SP-to-MC isomerization (thermocoloration). Other peptides also exhibited a quite similar photochromism involving the photobleaching and thermocoloration in neutral aqueous media (data not shown).

In order to obtain the kinetic parameters of spiropyran-containing peptides in neutral aqueous solution, relaxation (thermocoloration) processes from an SP-form to an equilibrium state (a mixture of SP- and MC-forms) in all peptides were followed by RP-HPLC to follow the progression of ring-opening reactions in the dark. Fig. 4 shows HPLC profiles of K-PKA-SP (**1**) incubated at 4 °C in the dark after exposure to ambient laboratory light to give the SP-form. A single peak was observed after 19 min in the chromatogram associated

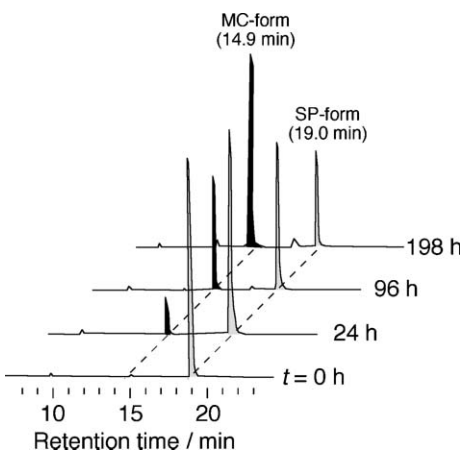

Fig. 4 HPLC profiles of K-PKA-SP (**1**) during the relaxation process from the SP- (grey line) to MC- (black line) forms acquired 0, 24, 96, and 198 h after starting incubation at 4 °C in the dark.

with an elapsed time of 0 h of thermocoloration in the dark and corresponding to the SP-form of the spiropyran moiety in the peptide. When the incubation was performed continuously the peak area of the SP-form after 19.0 min retention time decreased and a new peak at 14.9 min appeared corresponding to the pink sample solution. Each spiropyran-containing peptide showed characteristic increases in HPLC peak area with progression of the relaxation which depended on micro-environments of the spiropyran moiety in the peptide. Prolonged incubation (t > 200 h at 4 °C) caused decomposition of the spiropyran moiety in the peptides. Therefore, to obtain kinetic parameters the HPLC data were acquired within a 200 h time frame.

The kinetic parameters and equilibrium constants are summarized in Table 1. The SP-to-MC isomerization (thermocoloration) rate constants ($k_{SP\text{-}to\text{-}MC}$) vary between 2.3 and 6.7, and the MC-to-SP photoisomerization (photobleaching) rate constants ($k_{MC\text{-}to\text{-}SP}$) vary between 0.51 and 4.4, resulting in the equilibrium constants (K_{eq}) being in the range 0.52–6.1. These findings strongly support preferable stabilization of the zwitterion MC-forms in the peptides by solvation with bulk water molecules, as explained above. Nt-PKA-SP (**5**), in particular, showed the greatest K_{eq} constant at 6.1 (=3.1/0.51), probably due to the loss of mobility of the spiropyran moiety at the *N*-terminus of the peptide being different from that at side chains in the peptides. On the other hand, K-cSrc-SP (**6**) showed a reversed kinetic property in that the $k_{MC\text{-}to\text{-}SP}$ was greater than the $k_{SP\text{-}to\text{-}MC}$, resulting in a smaller K_{eq} constant, at 0.52, implying destabilization of the MC-form in the peptide. Although the net charge of the K-cSrc-SP (**6**) peptide sequence is +2, similar to those of the X-PKA-SP series (X = K, O, Db, Dp, and Nt, (**1–5**)), mutual repulsion of negative charges between the MC-form and the glutamic acid side chain in the sequence might affect the stabilization of the MC-form in K-cSrc-SP (**6**). These results suggest that the physicochemial properties in the SP-to-MC thermocoloration of spiropyran derivatives in aqueous media are strongly correlated with the micro-environments surrounding the spiropyran moieties in the peptides. Solution of the three dimensional structures of

Table 1 Physicochemical parameters in the photochromic properties of spiropyran-containing peptides[a]

Peptide	$10^3 k_{SP\text{-}to\text{-}MC}$/ h^{-1}	$10^3 k_{MC\text{-}to\text{-}SP}$/ h^{-1}	K_{eq}	Net charge
K-PKA-SP (**1**)	3.5	1.3	2.7	+/+ (+2)
O-PKA-SP (**2**)	5.6	2.2	2.5	+/+ (+2)
Db-PKA-SP (**3**)	6.7	2.9	2.3	+/+ (+2)
Dp-PKA-SP (**4**)	4.8	1.6	3.0	+/+ (+2)
Nt-PKA-SP (**5**)	3.1	0.51	6.1	+/+ (+2)
K-cSrc-SP (**6**)	2.3	4.4	0.52	−/+/+/+ (+2)
K-cAbl-SP (**7**)	4.6	1.6	2.9	+/+/+ (+3)
K-PKC-SP (**8**)	3.9	2.6	1.5	+/+/+/+ (+4)

[a] Physicochemical parameters were obtained from HPLC peak areas at retention times corresponding to the MC- and SP-forms in K-PKA-SP (**1**) (14.9 min/19.0 min for MC-/SP-forms); O-PKA-SP (**2**) (14.7/18.6); Db-PKA-SP (**3**) (14.6/18.4); Dp-PKA-SP (**4**) (14.7/18.4); Nt-PKA-SP (**5**) (14.7/18.8); K-cSrc-SP (**6**) (14.9/18.6); K-cAbl-SP (**7**) (14.5/18.4); K-PKC-SP (**8**) (13.6/17.4) under incubation conditions in 20 mM Tris HCl buffer (pH 7.4), 150 mM NaCl at 4 °C in the dark. The analytical procedure is described in the experimental section.

spiropyran-containing peptides by NMR would help in the understanding of the molecular details of such properties of spiropyran derivatives in aqueous media.

MC-to-SP photoisomerization properties of spiropyran-containing peptides

Next we examined the photophysical properties in the MC-to-SP photoisomerization (photobleaching) of the spiropyran-containing peptides. The fluorescence intensity of K-PKA-SP (**1**) at 600 nm was recorded as a function of irradiation time with 510 nm light in aqueous solution, giving a fluorescence decay curve that could be fitted with the following first-order equation, $F = F_\infty + (F_0 - F_\infty)\exp(-k_{\text{MC-to-SP}}t)$, where F is the fluorescence intensity at each time step, F_0 is the fluorescence intensity at $t = 0$ h, F_∞ is the fluorescence intensity of the SP-form, $k_{\text{MC-to-SP}}$ is the MC-to-SP photoisomerization rate constant, and t is the elapsed time under visible light irradiation (Fig. 5A). The photobleaching properties of MC-form in the K-PKA-SP (**1**) were investigated further. Fig. 5B shows the relative MC-to-SP photoisomerization rate constants as a function of the absorbance of the fluorescent MC-form at 510 nm in the sample solutions. In the case of absorbance ranging from 0.007 to 0.034, the peptide gave quite similar relative rate constants, but with an increase in absorbance to above 0.07, the relative rate constants tended to be sharply lowered, suggesting that analyses using the absorbance-independent region obtained above would be more suitable for highly reproducible results than analyses using the conventional fluorescence sensing systems. Furthermore, these findings also imply that protein–peptide interactions with a broad range of affinity constants would be detectable because the chemical structure of spiropyrans, controllable by UV light or irradiation or incubation in the dark, was independent of concentrations of the capturing peptides below 0.07 in absorbance.

In order to understand the MC-to-SP photobleaching in K-PKA-SP (**1**) in more depth, we measured photoisomerization rate constants under various conditions including 20% methanol in the buffer (v/v), *n*-hexanesulfonic acid sodium salt (n-$HexSO_3Na$), cetyl trimethylammonium bromide (CTAB), β-cyclodextrin (β-CD), and γ-cyclodextrin (γ-CD) (Fig. 6A). Neither negatively nor positively charged surfactants such as n-$HexSO_3Na$ and CTAB affected the MC-to-SP photoisomerization rate constants compared to those without additives. The addition of β-CD and γ-CD lowered the rate constants by 3.1% and 1.3%, respectively (negative effects).

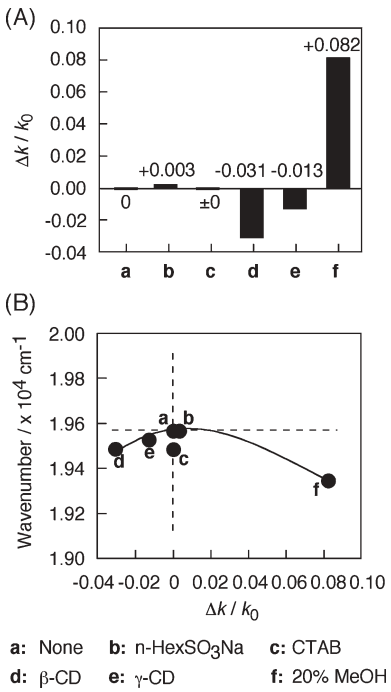

Fig. 6 (A) The positive/negative effects ($\Delta k/k_0$, $\Delta k = k - k_0$) in the MC-to-SP photoisomerization of K-PKA-SP (**1**) in the absence (k_0)/presence of n-$HexSO_3Na$, CTAB, β-CD, γ-CD, and MeOH ([K-PKA-SP (**1**)] = 2.2 μM, [n-$HexSO_3Na$], [CTAB], [β-CD], or [γ-CD] = 1.0 mM, [MeOH] = 20% in 20 mM Tris HCl buffer (pH 7.4), 150 mM NaCl at 4 °C. (B) The relationships between the MC-to-SP photoisomerization rate constants and absorption maxima.

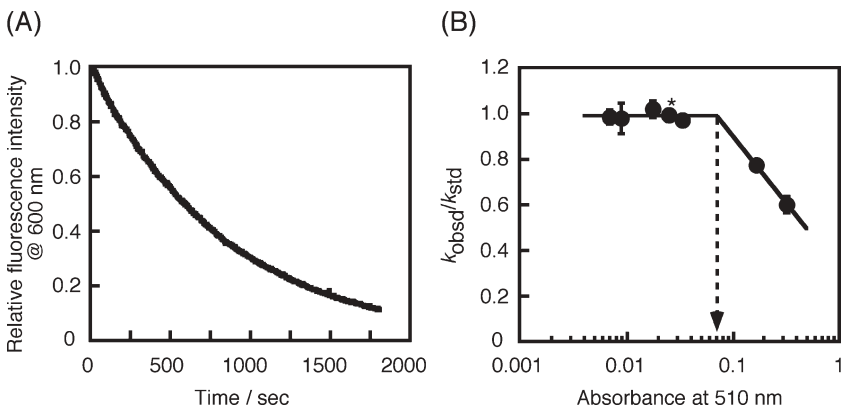

Fig. 5 (A) Fluorescence decay curve of K-PKA-SP (**1**) monitored at 600 nm obtained by irradiation of the sample solution with 510 nm light to photoisomerize from the MC- to SP-forms. The decay curve could be fitted with a simple first-order equation. [Peptide] = 2.2 μM and [PKA] = 0.76 mg mL^{-1} in 20 mM Tris HCl buffer (pH 7.4), 150 mM NaCl at 4 °C. (B) Concentration dependence of the MC-to-SP photoisomerization rate constants. Absorbance at 510 nm shows the concentration of the MC-form in the peptide. Samples of K-PKA-SP (**1**) ([peptide] = 0.14–28 μM) were irradiated with a 510 nm light in 20 mM Tris HCl buffer (pH 7.4), 150 mM NaCl at 4 °C. The standard photoisomerization rate constant is marked with an asterisk.

Meanwhile, the MC-to-SP photoisomerization in 20% methanol/buffer exhibited an increased rate constant by 8.2% (positive effects). Fig. 6B shows the relationships between the positive/negative effects in the photoisomerization and absorption bands of the MC-forms with various additives. The addition of CTAB, β-CD, γ-CD, and methanol shifted the absorption maxima of the MC-form to lower wavenumbers, indicating that the spiropyran moiety had been placed in reduced dielectric environments. In particular, β-CD and γ-CD provided not only reduced dielectric environments, but also sterically-hindered surroundings for the spiropyran moiety in the peptides by forming an inclusion complex.[34] These results indicated that the MC-to-SP photoisomerization was accelerated in solutions with lower dielectric constants (positive effects) and decelerated by sterically-hindered micro-environments (negative effects), motivating us to use the positive/negative effects in the MC-to-SP photoisomerization rate constants as a factor for the detection of target proteins.

Protein-peptide binding assay

We chose six different proteins: PKA, α-amylase, β-galactosidase, lysozyme, hexokinase, and S-100. Fig. 7A–F show the positive/negative effects in the photoisomerization of eight different spiropyran-containing peptides by the addition of the six different model proteins. The eight peptides gave characteristic patterns against model proteins: "+/−/+/−/+/+/+/−" for PKA, "−/−/−/−/−/+/0/−" for α-amylase, "−/−/−/−/+/+/+/−" for β-galactosidase, "−/−/−/−/−/+/+/−" for lysozyme, "−/+/+/+/+/−/+/−" for hexokinase, and "−/−/+/−/+/+/+/−" for S-100, with highly reproducible results. Protein fingerprints (a colored pattern for each protein) were created based on the positive/negative signals in the photoisomerization described above, in which the accelerated rate constants (positive effects) were expressed in red, the decelerated ones (negative effects) in green, and no effect in black (Fig. 7G). The resulting colored bar-code obtained for each protein was sufficiently unique to distinguish each protein from the others, suggesting that protein fingerprints based on the photoisomerization rate constants obtained by this P-CHROBA technique would be useful for profiling proteins. The P-CHROBA technique using the photoisomerization rate constants as a distinguishing factor has the advantage that background fluorescence signals from reagents do not affect the photobleaching of the MC-form during measurements because only the MC-form in the peptides is responsive to 510 nm light. Even the small number of spiropyran-containing peptides employed in the present study successfully distinguished between the target proteins. Increasing the size of a peptide library might improve the reliability for profiling numerous proteins.

K-PKA-SP (**1**) exhibited the positive and negative effects in photochromism on addition of 0.76 mg mL^{-1} of PKA and α-amylase, respectively (Fig. 7A and B), indicating that such photobleaching rate shifts were associated with the properties of the binding between proteins and peptides. We further investigated relationships between the protein concentration and the MC-to-SP photoisomerization rate constants to extend the applicability of the P-CHROBA technique. Fig. 7H shows

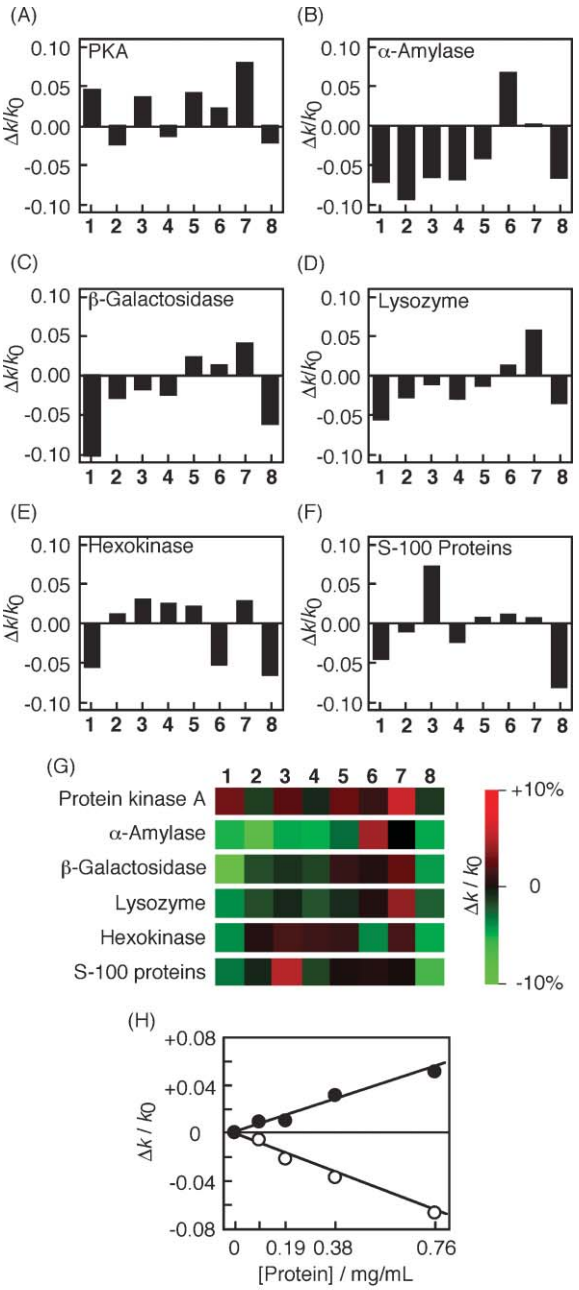

Fig. 7 (A)–(F) Data for the positive/negative effects ($\Delta k/k_0$, $\Delta k = k - k_0$) in the MC-to-SP photoisomerization rate constants on addition of the six different target proteins. Peptides ([peptide] = 2.0–2.2 μM) were irradiated with 510 nm light in the presence and absence of proteins ([protein] = 0.76 mg mL^{-1}) to give the MC-to-SP photoisomerization rate constants, k and k_0 in 20 mM Tris HCl buffer (pH 7.4), 150 mM NaCl at 4 °C, respectively. Experimental errors were estimated to be mostly within ±2.0%. (G) The protein fingerprints created on the basis of the positive/negative effects obtained in Fig. 7A–F. The positive and negative effects are red and green, respectively. (H) Changes in the MC-to-SP photoisomerization rates of K-PKA-SP (**1**) depending upon concentrations of PKA (closed circles) and α-amylase (open circles). [K-PKA-SP (**1**)] = 2.2 μM, [protein] = 0, 0.095, 0.19, 0.38, and 0.76 mg mL^{-1} in 20 mM Tris HCl buffer (pH 7.4), 150 mM NaCl at 4 °C.

the dependence of the accelerated/decelerated photoisomerization rate constants of K-PKA-SP (**1**) on the concentrations of PKA and α-amylase. The protein concentrations varying from 0 to 0.76 mg mL^{-1} gave a linear correlation between $\Delta k/k_0$ and the protein concentrations. With increasing PKA concentration, the photoisomerization accelerated linearly, conversely the addition of α-amylase reduced the $\Delta k/k_0$ values, indicating that the P-CHROBA technique, using the working curves based on the $\Delta k/k_0$ values, is applicable to the quantification of protein concentrations. However, the method showed relatively high detection limits, indicating that it still requires further development to become a practical technique. Although analytical methods utilizing fluorescent probes are generally quite sensitive, it is relatively difficult to provide reproducible results and reduce background signals from excess reagents. The present technique can solve such difficulties because it is based on measurement of the MC-to-SP photoisomerization rate constants. These values can be stabilized if fluorescence decay curves are acquired under the standard conditions, and the method can avoid the need for immobilization of capture agents onto solid surfaces, facilitating removal of excess reagents. Furthermore, combination of the P-CHROBA and PFP techniques would be one of the most versatile analytical tools for proteomic studies.

Conclusions

In the present study we have described the synthesis and characterization of photochromic spiropyran-containing peptides, and the feasibility of a unique fluorescence sensing system based on the photochromic properties of the peptides (P-CHROBA). The spiropyran moiety in the peptides exhibited characteristic physicochemical properties in SP-to-MC isomerization (thermocoloration) and MC-to-SP photoisomerization (photobleaching) which depend on changes in the micro-environment such as the dielectric constant of the solvent and steric hindrances generated by interactions. The MC-to-SP photobleaching of the MC-form in the peptides was faster than the SP-to-MC thermocoloration in neutral aqueous media. Thus, we successfully demonstrated the use of photobleaching-process-shifts resulting from protein–peptide interactions, which can leas to reduced background fluorescence signals from excess reagents, avoid laborious introduction of probing molecules to analytes, and omit the need for immobilization of capture agents onto solid surfaces. The PFP technique using peptides also had the advantages that short peptides are (i) easy to prepare and (ii) responsive enough to distinguish between target proteins by a colored bar-code based on changes in fluorescence decay curves, even though they bind relatively poorly to proteins. The combination of the P-CHROBA and PFP techniques would provide a powerful tool for profiling target proteins with reproducible and reliable results.

Experimental

General

Absorption spectra were acquired on a Shimadzu UV-2550 spectrophotometer equipped with a thermoregulator using a quartz cell (10 mm path length) at various temperatures. Fluorescence spectra were aquired on a Hitachi F-2500 fluorescence spectrophotometer equipped with a magnetic stirrer and a thermoregulator using a quartz cell (5.0 mm in width × 10 mm in path length) at various temperatures. All proteins (PKA, α-amylase, β-galactosidase, lysozyme, hexokinase, and S-100) were purchased from Sigma-Aldrich, Japan. All solvents and reagents (except amino acid derivatives) were purchased from Wako Pure Chemical Industries (Osaka, Japan) and used as received. Fmoc-amino acid derivatives including Fmoc-Orn(Boc)-OH, Fmoc-Dab-OH, and Fmoc-Dap-OH were purchased from Watanabe Chemical Industries (Hiroshima, Japan). Acetonitrile (HPLC grade) was used for the HPLC analysis and purification.

Chromatography

Adsorption column chromatography was performed using flash silica gel (70–230 mesh, Merck). Analytical HPLC and purification of the peptides were performed on a Hitachi L7000 or a Shimadzu LC2010C system equipped with a Wakosil 5C18 or a YMC-pack ODS-A (4.6 × 150 mm) with a linear gradient of acetonitrile/0.1% TFA at a flow rate of 1.0 mL min^{-1} for analysis, and a YMC ODS A323 (10 × 250 mm) at a flow rate of 3.0 mL min^{-1} for preparative purification.

Mass spectrometry

Mass spectra were obtained by matrix-assisted laser desorption/ionization time-of-flight mass spectrometry (MALDI-TOFMS, KOMPACT MALDI III, Shimadzu, Japan) with 3,5-dimethoxy-4-hydroxycinnamic acid (SA) as the matrix.

Non-commercial compounds

2-(3′,3′-Dimethyl-6-nitro-3′*H*-spiro[chromene-2,2′-indole]-1′-yl)ethanol (**9**) was prepared as described in the literature.[25]

p-Nitrophenyl 2-(3′,3′-dimethyl-6-nitro-3′*H*-spiro[chromene-2,2′-indole]-1′-yl)ethylcarbonate (10)

A solution of *p*-nitrophenyl chloroformate (572 mg, 2.84 mmol) in CH_2Cl_2 (5.0 mL) was added to a mixture of **9** (1.00 g, 2.84 mmol) and diisopropylethylamine (DIEA, 2.0 mL) in CH_2Cl_2 (20 mL) dropwise for 1 min at 0 °C and the resulting reaction mixture was stirred at 0 °C continuously. After 1 h, the addition of the solution of *p*-nitrophenyl chloroformate (572 mg, 2.84 mmol) in CH_2Cl_2 (5.0 mL) was repeated and the mixture was stirred at 0 °C. After 1 h, another solution of *p*-nitrophenyl chloroformate (572 mg, 2.84 mmol) in CH_2Cl_2 (5.0 mL) was added and the resulting mixture was stirred at 0 °C. After 1 h, the reaction mixture was concentrated and purified by column chromatography [silica, ethyl acetate/petroleum ether (1 : 2)]. The residue was decanted with diethyl ether/petroleum ether twice, followed by vacuum filtration, giving a faintly pink solid (827 mg, 56%): mp 99–101 °C (dec). Analytically calculated for $C_{27}H_{23}N_3O_8$: C, 62.67; H, 4.48; N, 8.12. Found: C, 61.53; H, 4.56; N, 7.98.

L-α-(9-Fluorenylmethoxycarbonyl)-ω-[2-(3′,3′-dimethyl-6-nitro-3′*H*-spiro[chromene-2,2′-indole]-1′-yl)ethoxycarbonyl]ornithine (Fmoc-Orn(SP)-OH, 11)

Fmoc-Orn(Boc)-OH (175 mg, 0.386 mmol) was treated with TFA (3.0 mL) at 0 °C for 30 min. The reaction mixture was concentrated, precipitated from diethyl ether/petroleum ether, and dried *in vacuo*, giving a colorless solid. The solid was reacted with **10** (100 mg, 0.193 mmol) in the presence of DIEA (134 μL, 0.772 mmol) in *N,N*-dimethylformamide (DMF, 5.0 mL) at 0 °C for 30 min then at room temperature for 1 h. Ethyl acetate was added to the reaction mixture, and the organic phase was washed with 10% citric acid and water and dried over $MgSO_4$. Silica gel column chromatography [$CHCl_3$/methanol/acetic acid (90/10/10)] followed by precipitation from diethyl ether/petroleum ether gave a faintly yellowish solid (57 mg, 40%): mp 114–116 °C (dec); MALDI-TOFMS (SA) observed, 733.4 $[M + H]^+$; calculated, 732.8. Calculated for $C_{41}H_{40}N_4O_9 + 3H_2O$: C, 61.18; H, 6.02; N, 6.96. Found: C, 61.35; H, 5.51; N, 6.81.

L-α-(9-Fluorenylmethoxycarbonyl)-ω-[2-(3′,3′-dimethyl-6-nitro-3′*H*-spiro[chromene-2,2′-indole]-1′-yl)ethoxycarbonyl]-diaminobutyric acid (Fmoc-Dab(SP)-OH, 12)

Following the general method described in the synthesis of compound **11**, Fmoc-Dab-OH (79.0 mg, 0.232 mmol) was reacted with **10** (100 mg, 0.193 mmol) in the presence of DIEA (81 μL, 0.464 mmol) in DMF (10 mL) at 0 °C for 30 min, then at room temperature for 5 h. Chromatographic purification followed by precipitation from diethyl ether/petroleum ether gave a faintly orange solid (95 mg, 68%): mp 114–116 °C (dec); MALDI-TOFMS (SA) observed, 718.4 $[M + H]^+$; calculated, 718.8. Calculated for $C_{40}H_{38}N_4O_9 + H_2O$: C, 65.21; H, 5.47; N, 7.60. Found: C, 65.74; H, 5.40; N, 7.56.

L-α-(9-Fluorenylmethoxycarbonyl)-ω-[2-(3′,3′-dimethyl-6-nitro-3′*H*-spiro[chromene-2,2′-indole]-1′-yl)ethoxycarbonyl]-diaminopropionic acid (Fmoc-Dap(SP)-OH, 13)

Following the general method described in the synthesis of compound **11**, Fmoc-Dap-OH (80.0 mg, 0.232 mmol) was reacted with **10** (100 mg, 0.193 mmol) in the presence of DIEA (81 μL, 0.464 mmol) in DMF (3.0 mL) at 0 °C for 30 min, then at room temperature for 3 h. Chromatographic purification followed by precipitation from diethyl ether/petroleum ether gave a faintly yellowish solid (83 mg, 61%): mp 118–121 °C (dec); MALDI-TOFMS (SA) observed, 704.6 $[M + H]^+$; calculated, 704.7. Calculated for $C_{39}H_{36}N_4O_9 + 2H_2O$: C, 63.24; H, 5.44; N, 7.56. Found: C, 63.27; H, 5.22; N, 7.44.

General procedure of preparation of the spiropyran-containing peptides (Route 1)

Peptides were synthesized by means of Fmoc chemistry on Rink amide MBHA resin with 2-(1*H*-benzotriazole-1-yl)-1,1,3,3-tetramethyluronium hexafluorophosphate (HBTU) and 1-hydroxybenzotriazole monohydrate (HOBt) as coupling reagents.[33,35] The side chains of the amino acids were protected as follows: acetamidomethyl (Acm) for Cys, *t*-butyloxycarbonyl (Boc) or 4-methyltrityl (Mtt) for Lys, 2,2,4,6,7-pentamethyldihydrobenzofurane-5-sulfonyl (Pbf) for Arg, *t*-butyl ester (O^tBu) for Glu, and *t*-Bu ether (^tBu) for Tyr, Thr, and Ser. Initially the Ac–Cys(Acm)–Gly–Lys(Mtt)–Gly–[various sequences]–Gly resin was prepared in 30 μmol quantities. The peptide-bound resin was dried *in vacuo* and divided into two portions. Half of the peptide-bound resin (15 μmol) was treated with TFA/TIS/CH_2Cl_2 (1/5/94, v/v/v) at room temperature to remove the Mtt protecting group of the Lys residue. The resulting peptide-bound resin was washed with 1% DIEA/*N*-methyl-2-pyrrolidone (NMP) (three times), then neat NMP (three times) and treated with **10** (3 eq) and DIEA (6 eq) at room temperature in the dark. After 6 h, DIEA (6 eq) was added again and the reaction mixture was shaken at room temperature in the dark. After 12 h the reaction mixture was filtered and washed with NMP then $CHCl_3$. All of the protecting groups except Acm were removed by the treatment of TFA/*m*-cresol/EDT/TA (40/1/3/3, v/v/v/v) for 1 h at room temperature. The crude peptide obtained was purified by RP-HPLC and characterized by MALDI-TOFMS (SA), giving a fluffy yellow powder: K-PKA-SP (**1**, 6.7 mg, 28%): observed, 1608.5 $[(M + H)^+]$; calculated 1607.8. K-cSrc-SP (**6**, 5.6 mg, 19%): observed, 1929.0 $[(M + Na)^+]$, 1906.1 $[(M + H)^+]$; calculated, 1905.2. K-cAbl-SP (**7**, 6.7 mg, 25%): observed, 1834.1 $[(M + Na)^+]$, 1813.3 $[(M + H)^+]$; calculated 1811.1. K-PKC-SP (**8**, 4.6 mg, 18%): observed, 1723.4 $[(M + H)^+]$; calculated 1722.0.

General procedure of preparation of the spiropyran-containing peptides (Route 2)

The fully-protected peptide-bound resins were prepared and deprotected/deresinated by the general method described above. The crude peptide obtained was purified by RP-HPLC and characterized by MALDI-TOFMS (SA), affording a fluffy yellow powder: O-PKA-SP (**2**, 1.8 mg, 3.6%): observed, 1596.8 $[(M + H)^+]$; calculated, 1593.8. Db-PKA-SP (**3**, 1.8 mg, 3.8%): observed, 1582.3 $[(M + H)^+]$; calculated 1579.8. Dp-PKA-SP (**4**, 1.9 mg, 4.0%): observed, 1566.6 $[(M + H)^+]$; calculated 1565.8.

General procedure of preparation of the spiropyran-containing peptides (Route 3)

The fully-protected Fmoc–Cys(Acm)–Gly–Ala–Gly–Leu–Arg(Pbf)–Arg(Pbf)–Ser(^tBu)–Leu–Gly–resin was prepared by the general method described above. The Fmoc protecting group at the *N*-terminus was removed with 20% piperidine/NMP and washed with NMP **10** (47 mg, 90 μmol). It was reacted with the amino group in the peptide on resin in the presence of DIEA (31 μL, 0.18 mmol) in NMP. After 2 h, DIEA (31 μL, 0.18 mmol) was added and the resulting mixture was shaken overnight. The peptide-bound resin was treated with TFA/*m*-cresol/EDT/TA (40/1/3/3, v/v/v/v) for 1 h at room temperature. The crude peptide obtained was purified by RP-HPLC and characterized by MALDI-TOFMS (SA), giving a fluffy yellow powder: Nt-PKA-SP (**5**, 3.3 mg, 7.3%) observed, 1509.9 $[(M + H)^+]$; calculated 1508.7.

Thermally equilibrium studies of the spiropyran-containing peptides

The peptide solution (300 μM) in a 20 mM Tris HCl buffer containing 150 mM NaCl (pH 7.4) was irradiated in ambient laboratory light at 4 °C for 30 min to convert it to the SP-form. An aliquot (10 μL) was removed from the peptide solution and evaluated by RP-HPLC (with a linear gradient of 0–100% acetonitrile/0.1% TFA at a flow rate of 1.0 mL min^{-1} for 30 min detected at 300 nm) as a HPLC chromatogram at $t = 0$ h. The solution was incubated at 4 °C in the dark and evaluated by RP-HPLC at each time step. The increasing and decreasing HPLC peak areas of the MC- and SP-forms, respectively, were plotted and fitted with the following equation to obtain the thermodynamic parameters, $A = A_\infty + (A_0 - A_\infty)\exp(-\tau^{-1}t)$, where A is the peak area of the MC-/SP-form in a HPLC chromatogram at each time step, A_0 is the peak area of the MC/SP-form at $t = 0$ h, A_∞ is the peak area of the MC-/SP-form in an equilibrium state, τ is the relaxation constant ($\tau^{-1} = k_{\text{SP-to-MC}} + k_{\text{MC-to-SP}}$), and t is the time elapsed. The equilibrium constants (K_{eq}) were calculated from the equation, $K_{eq} = [\text{MC}]/[\text{SP}] = A_\infty(\text{MC})^c/A_\infty(\text{SP})^c$, where $A_\infty(\text{MC})^c$ and $A_\infty(\text{SP})^c$ are corrected peak areas in an equilibrium state [calculated from the following relation, $A_\infty(\text{MC}) - A_0(\text{MC}) = A_0(\text{SP}) - A_\infty(\text{SP})$]. Finally, both $k_{\text{SP-to-MC}}$ and $k_{\text{MC-to-SP}}$ were calculated by the following equations, $\tau^{-1} = k_{\text{SP-to-MC}} + k_{\text{MC-to-SP}}$ and $K_{eq} = k_{\text{SP-to-MC}}/k_{\text{MC-to-SP}}$.

Kinetic studies of the MC-to-SP photoisomerization

A sample solution of a spiropyran-containing peptide with or without a protein of interest in 20 mM Tris HCl buffer containing 150 mM NaCl (pH 7.4) was incubated overnight at 4 °C in the dark. The sample was transferred to a quartz cell (5.0 × 10 mm) placed at the thermoregulator in the Hitachi F-2500 fluorescence spectrophotometer, and stirred with a magnetic bar at a desired temperature for 30 min before measurement was started. The fluorescence decay of MC species at 600 nm (excitation at 510 nm) was detected after a time of 1800 s. The fluorescence decay curve obtained was fitted with the first-order kinetic equation, $F = F_\infty + (F_0 - F_\infty)\exp(-k_{\text{MC-to-SP}}t)$ and analyzed by KaleidaGraph software (Synergy Software), where F is the fluorescence intensity at each time step, F_∞ is the fluorescence intensity at infinity, F_0 is the initial fluorescence intensity, $k_{\text{MC-to-SP}}$ is the MC-to-SP photoisomerization rate constant, and t is the elapsed time.

Kin-ya Tomizaki and Hisakazu Mihara*
Department of Bioengineering and the COE21 Program, Graduate School of Bioscience and Biotechnology, Tokyo Institute of Technology, B-40, 4259 Nagatsuta, Midori, Yokohama 226-8501, Japan.
E-mail: hmihara@bio.titech.ac.jp; Fax: +81-45-924-5833

References

1 (*a*) R. J. Lipshutz, S. P. Fodor, T. R. Gingeras and D. J. Lockhart, *Nat. Genet.*, 1999, **21**, 20–24; (*b*) D. A. Lashkari, J. L. DeRisi, J. H. McCusker, A. F. Namath, C. Gentile, S. Y. Hwang, P. O. Brown and R. W. Davis, *Proc. Natl. Acad. Sci. USA*, 1997, **94**, 13057–13062.
2 (*a*) *Protein Microarray Technology*, ed. D. Kambhampati, Wiley-VCH, Weinheim, 2003; (*b*) *Protein Arrays: Methods and Protocols; Methods in Molecular Biology*, ed. E. T. Fung, Humana Press, New Jersey, 2004, **vol. 264**.
3 G. Walter, K. Büssow, D. Cahill, A. Lueking and H. Lehrach, *Curr. Opin. Microbiol.*, 2000, **3**, 298–302.
4 H. Zhu and M. Snyder, *Curr. Opin. Chem. Biol.*, 2001, **5**, 40–45.
5 T. Kodadek, *Chem. Biol.*, 2001, **8**, 105–115.
6 Y.-S. Lee and M. Mrksich, *Trends Biotechnol.*, 2002, **20**, 12 suppl., S14–S18.
7 B. Schweitzer and S. F. Kingsmore, *Curr. Opin. Biotechnol.*, 2002, **13**, 14–19.
8 M. Yanagida, *J. Chromatogr. B*, 2002, **771**, 89–106.
9 M. F. Templin, D. Stoll, M. Schrenk, P. C. Traub, C. F. Vöhringer and T. O. Joos, *Trends Biotechnol.*, 2002, **20**, 160–166.
10 M. F. Lopez and M. G. Pluskal, *J. Chromatogr. B*, 2003, **787**, 19–27.
11 H. Zhu and M. Snyder, *Curr. Opin. Chem. Biol.*, 2003, **7**, 55–63.
12 J. Glökler and P. Angenendt, *J. Chromatogr. B*, 2003, **797**, 229–240.
13 A. Bradbury, N. Velappan, V. Verzillo, M. Ovecka, L. Chasteen, D. Sblattero, R. Marzari, J. Lou, R. Siegel and P. Pavlik, *Trends Biotechnol.*, 2003, **21**, 312–317.
14 D. S. Wilson and S. Nock, *Angew. Chem. Int. Ed.*, 2003, **42**, 494–500.
15 D. N. Howbrook, A. M. van der Valk, M. C. O'Shaughnessy, D. K. Sarker, S. C. Baker and A. W. Lloyd, *Drug Discovery Today*, 2003, **8**, 642–651.
16 S. Hanash, *Proteomics*, 2003, **3**, 2075–2076, special issue on Protein Microarrays.
17 K.-Y. Tomizaki, K. Usu and and H. Mihara, *ChemBioChem*, **6**, DOI: 10.1002/cbic.200400232.
18 http://www.invitrogen.com.
19 http://www.protometrix.com.
20 K. Usui, M. Takahashi, K. Nokihara and H. Mihara, *Mol. Diversity*, 2004, **8**, 209–218.
21 K. Usui, T. Ojima, M. Takahashi, K. Nokihara and H. Mihara, *Biopolymers*, 2004, **76**, 129–139.
22 M. Takahashi, K. Nokihara and H. Mihara, *Chem. Biol.*, 2003, **10**, 53–60.
23 (*a*) G. Berkovic, V. Krongauz and V. Weiss, *Chem. Rev.*, 2000, **100**, 1741–1753; (*b*) N. Tamai and H. Miyasaka, *Chem. Rev.*, 2000, **100**, 1875–1890.
24 J. B. Flannery, Jr., *J. Am. Chem. Soc.*, 1968, **90**, 5660–5671.
25 (*a*) F. M. Raymo and S. Giordani, *J. Am. Chem. Soc.*, 2001, **123**, 4651–4652; (*b*) F. M. Raymo and S. Giordani, *J. Am. Chem. Soc.*, 2002, **124**, 2004–2007.
26 J. Sunamoto, K. Iwamoto, Y. Mohri and T. Kominato, *J. Am. Chem. Soc.*, 1982, **104**, 5502–5504.
27 B. I. Ipe, S. Mashima and K. G. Thomas, *J. Am. Chem. Soc.*, 2003, **125**, 7174–7175.
28 A. Shumburo and M. C. Biewer, *Chem. Mater.*, 2002, **14**, 3745–3750.
29 K.-Y. Tomizaki, J. Xu and H. Mihara, *Bioorg. Med. Chem. Lett.*, 2005, **15**, 1731–1735.
30 S. Cox and S. S. Taylor, *Biochemistry*, 1995, **34**, 16203–16209.
31 B. T. Houseman, J. H. Huh, S. J. Kron and M. Mrksich, *Nat. Biotechnol.*, 2002, **20**, 270–274.
32 L. E. Heasley and G. L. Johnson, *J. Biol. Chem.*, 1989, **264**, 8646–8652.
33 *Fmoc Solid Phase Peptide Synthesis: A Practical Approach*, ed. W. C. Chen and P. D. White, Oxford University Press, New York, 2000.
34 F. Hamada, K. Hoshi, Y. Higuchi, K. Murai, Y. Akagami and A. Ueno, *J. Chem. Soc., Perkin Trans. 2*, 1996, 2567–2570.
35 R. Knorr, A. Trzeciak, W. Bannwarth and D. Gillessen, *Tetrahedron Lett.*, 1989, **30**, 1927–1930.

